A full scale hydrodynamic simulation of detonation and deflagration in an energetic component system

Bohoon Kim and Jack J. Yoh*
Department of Mechanical and Aerospace Engineering, Seoul National University
Seoul, Korea 151-742

1 Introduction

The analysis of pyrotechnic mechanical actuation requires a full-scale, fully-integrated dynamic simulation of fluid-solid, combustion of explosives and propellants in a train configuration. The reaction of a solid-phase energetic material must be precisely calculated before transferring subsequent dynamic loading onto a contacting inert structure such as a metal or plastic that is commonly in contact with another energetic material in a so called train configuration. A pyrotechnic mechanical device (PMD) is typically devised with several energetic components together with inert gap materials that often play the role of shock pressure attenuator for various applications. Airbag inflator is a common example that relies on this multi-material energetic-inert composite design that ultimately works as a single system to achieve rapid release of high pressure gas intended for inflating the airbag for automobile safety, for instance.

One needs to adapt a stable, multi-material interface handling algorithm based on a strongly-coupled fluid-structure interaction framework while accurately solving the chemical response of the involved high explosives, propellants, and reactive (powder) components. In addition, the equations of state for each energetic material as well as the inert materials need to be modeled to reproduce the full scale test of the energetic system in a train configuration.

In this research, we attempt to conduct a full-scale numerical simulation of a multi-material pyrotechnic combustion that involves detonation of a composite donor (HNS+HMX), high pressure attenuation in a gap (stainless steel), detonation of an acceptor (RDX), and finally a deflagration of a gas-generating propellant ($BKNO_3$) using a house code. The present train configuration of two-dimensional layers of energetic-inert materials is designed for purging high pressure gas into a 10 cc dump chamber for subsequent monitoring of the flow oscillation due to inherent shock and rarefactions. A closed bomb test is also used to validate the full-scale simulation results provided in the study.

2 Numerical approach

Correspondence to: jjyoh@snu.ac.kr

In order to simulate the energetic responses of high explosives and propellant contained in a donor-acceptor arrangement in stainless steel casing, the mathematical formulation is required to include reactive 9flow models for both detonation and deflagration, rupture model for metal, multi-material interface tracking model, and hydrodynamic model for accurate capturing of various acoustic waves inherent to a globally hyperbolic system. The dynamic response of both energetic and inert components of the given system is described by the compressible form of the governing equations, and the stress tensor that describes the structural response of steel is comprised of a deviatoric stress and a hydrostatic pressure. The Mie-Gruneisen equation of state (EOS) defines the pressure attained by the gap between donor-acceptor high explosive pair, while the Jones-Wilkins-Lee (JWL) EOS determines explosive pressure resulting from the hydro-thermodynamic state. The rate of chemical reaction is based on the ignition and growth kinetics [1]. The material interface between any two materials is tracked through a hybrid particle level set method, while material properties in the vicinity of an interface are determined through the ghost fluid method [2].

The compressible Navier-Stokes equations in two-dimensional system reflect the conservations of mass, momentum and energy:

$$\frac{\partial \vec{U}}{\partial t}+\frac{\partial \vec{E}}{\partial r}+\frac{\partial \vec{F}}{\partial z}=\vec{S}\left(\vec{U}\right) \tag{1}$$

$$\vec{U}=\begin{bmatrix}\rho\\ \rho u_r\\ \rho u_z\\ \rho E\end{bmatrix},\quad \vec{E}=\begin{bmatrix}\rho u_r\\ \rho u_r^2+p\\ \rho u_r u_z\\ u_r(\rho E+p)\end{bmatrix},\quad \vec{F}=\begin{bmatrix}\rho u_z\\ \rho u_z u_r\\ \rho u_z^2+p\\ u_z(\rho E+p)\end{bmatrix} \tag{2}$$

$$\vec{S}=\begin{bmatrix}-\dfrac{\rho u_r}{r}\varphi\\ \dfrac{s_{rr}-s_{\theta\theta}-\rho u_r^2}{r}\varphi+\eta\left(\dfrac{\partial s_{rr}}{\partial r}+\dfrac{\partial s_{zr}}{\partial z}\right)\\ \dfrac{s_{zr}-\rho u_r u_z}{r}\varphi+\eta\left(\dfrac{\partial s_{rz}}{\partial r}+\dfrac{\partial s_{zz}}{\partial z}\right)\\ \dfrac{u_r s_{rr}+u_z s_{rz}-u_r(\rho E+p)}{r}\varphi+\eta\left(\dfrac{\partial (u_r s_{rr}+u_z s_{rz})}{\partial r}+\dfrac{\partial (u_r s_{zr}+u_z s_{zz})}{\partial z}\right)\end{bmatrix} \tag{3}$$

where $\varphi = 0$ for rectangular and $\varphi = 1$ for cylindrical coordinates. Also, $\eta = 0$ for energetic materials while $\eta = 1$ for inert (metal) materials. The source term refers to the governing tensor for the structure. The resulting hyperbolic system of equations is solved by a third-order Runge-Kutta and ENO (essentially non-oscillatory) methods for temporal and spatial discretizations, respectively. Here, stress effect in the unreacted high explosives or propellant is ignored in comparison to a dominantly high hydrostatic pressure resulted from the reacted product gases. The sharpness of the interface between any two different materials is guaranteed by applying the hybrid particle level set method as outlined in [2].

In describing both unreacted and product states of an energetic material, the equations of state defining the pressure are utilized. The Jones-Wilkins-Lee (JWL) form [3] of Eqs. (4) and (5) are used.

$$p_{unreacted} = A\left(1-\frac{\omega}{R_1(\rho_0/\rho)}\right)e^{-R_1(\rho_0/\rho)} + B\left(1-\frac{\omega}{R_2(\rho_0/\rho)}\right)e^{-R_2(\rho_0/\rho)} + \frac{\omega e_0}{(\rho_0/\rho)} \tag{4}$$

$$p_{reacted} = Ae^{-R_1(\rho_0/\rho)} + Be^{-R_2(\rho_0/\rho)} + \frac{C}{(\rho_0/\rho)^{\omega+1}} \tag{5}$$

ρ_0 and ρ are the initial and current densities, respectively. A, B, C, R_1, and R_2 are the material dependent JWL parameters with ω being the Gruneisen coefficient. These parameters are obtained by fitting the JWL EOS to the cylinder expansion test results or thermodynamic equilibrium calculation of CHEETAH 2.0 [4], where $e_0 = \rho_0 C_v T$ refers to the thermodynamic energy in GPa. In particular, Eq. (5) is an isentropic JWL C-term form of EOS used for gaseous products.

The reactive flow model is described by the rate law that consists of both ignition and growth terms suggested by Kim et al. [1]

$$\frac{d\lambda}{dt} = I(1-\lambda)\mu^a + G(1-\lambda)p^b \qquad \mu = \frac{\rho}{\rho_0} - 1 \tag{6}$$

Here, t is time, λ is the burned mass fraction, and constants I, a, G, b are the unknown parameters. λ represents reaction progress where $\lambda = 0$ is unreacted and $\lambda = 1$ is reacted state. The compression, μ, is defined $\mu = \rho/\rho_0$-1. Four unknown parameters of major significance in view of detonation are determined by a series of standardized unconfined rate stick experiment performed [1].

For the RDX, the constants of ignition I and growth G were set at 5.8×10^7 s^{-1} and 3.8×10^8 s^{-1}Mbar^{-b}, respectively. The pressure sensitivity b was 1.1, and the compression sensitivity a was 4.0.

$$\frac{d\lambda}{dt} = I(1-\lambda)^{0.222}\mu^a + G(1-\lambda)\lambda^{0.666}p^b \tag{7}$$

The rate law of HMX was modeled by Eq. (7), with the rate parameters of $I = 4.4\times10^7$ s^{-1}, $a = 4.0$, $G = 8.5\times10^8$ s^{-1}Mbar^{-b}, and $b = 2.0$.

The chemical reaction of $BKNO_3$ corresponds to deflagration and the reaction rate is calculated as follows.

$$\frac{d\lambda}{dt} = \sqrt{\frac{Z\cdot e^{-E_a/(\bar{R}T)}\cdot k\cdot \bar{R}T_f^2}{c_p\cdot E_a\cdot(T_f - T_0)}}\Big/\rho_0 \tag{8}$$

Here, the thermal response is simulated using the Arrhenius law, and related parameters are quantified by the calorimetry [5]. $\bar{R}$ is the universal gas constant, c_p and T_f are constant pressure coefficient of heat and flame temperature of propellant, respectively. The reaction parameters of $BKNO_3$ are $Z = 9.2\times10^9$ s^{-1}, $E_a = 1.8\times10^5$ kJ/kmol, and $k = 3.2\times10^{-3}$ kJ/m-sec-K.

3 Simulation results

The closed bomb test (CBT) provides the measured chamber pressure when $BKNO_3$ is deflagrated to release hot product gas into a 10 cc purge chamber. Figure 1 shows the pyrotechnic initiator-chamber assembly on the left and the computational domain on the right. The primary layer of donor is HNS (hexanitrostilbene, $C_{14}H_6N_6O_{12}$) with an initial density of 1.43 g/cc. The next layer is HMX

(cyclotetramethylene-tetranitramine, $C_4H_8N_8O_8$) with initial density of 1.70 g/cc. The electrical flyer initiator is used to ensure the ignition of the layered donor assembly. Separated by the bulkhead or gap of stainless steel 304, acceptor charge is of 97.5% RDX by weight. The donor-gap-acceptor train configuration is then utilized to ignite the boron potassium nitrate ($BKNO_3$) of 1.3 g/cc for uniform gas generation into the chamber.

The numerical simulation requires a large number of meshes through the reactive area of the explosive material, in order to resolve the sharp detonation structure and to attain the theoretical C-J equilibrium properties. The SDT calculation is both mesh and time intensive as the velocity on the order of several thousand meters per second and few tens of GPa in pressure are generated within microscale widths of RDX and HMX reaction zones. Specifically, the reaction zone width is approximately 0.1 mm for HMX and 0.5 mm for RDX. We selected the mesh size of 0.01 mm × 0.01 mm for the integrated system simulation in the rest of the study.

A pressure sensor measures the central wall pressure fluctuation during the event, as the sensor is of the model #102B of PCB piezotronics which is connected to ICP model 484b signal conditioner and receives the voltage signal with a DAQ system. In order to observe the initial reaction of the assembly, the sampling rate was measured for precision up to 2000 μs at 20 GHz as shown in Fig. 2. Raw data and the low-pass filtered pressure measurement are shown. The pressure perturbation is clearly observed in the downstream. From the results, it can be seen that the combustion gas of $BKNO_3$ flow into the CBT chamber when the pressure rises at about 100 μs from the start of the explosion. After 500 μs, we can observe a swirling flow which seems to be due to the propagation of oscillating reacting waves in the CBT interior space. The Fast Fourier Transform results obtained by converting the pressure signal with time into the frequency domain are shown in Fig. 3. The observed frequency was about ω_c = 8.3 kHz. This particular frequency is due to the time characteristics of the oscillating flow bouncing inside the chamber.

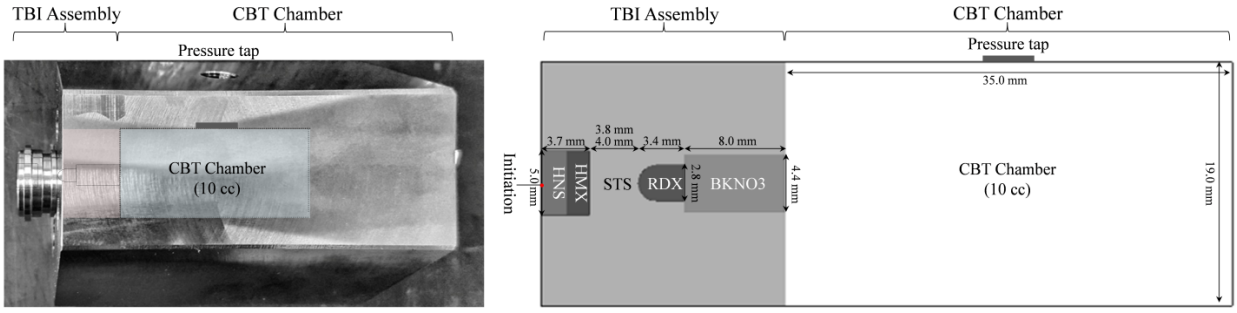

Figure 1. Test specimen (left) and computational domain (right) for closed bomb test

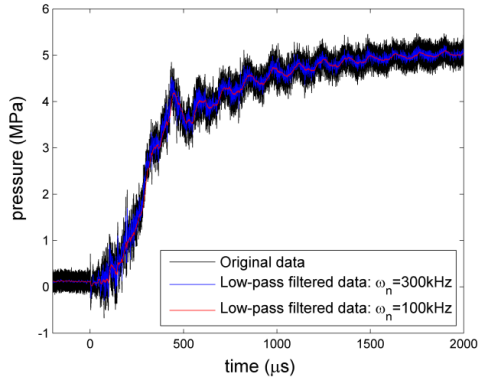

Figure 2. Measured raw and filtered pressure CBT data

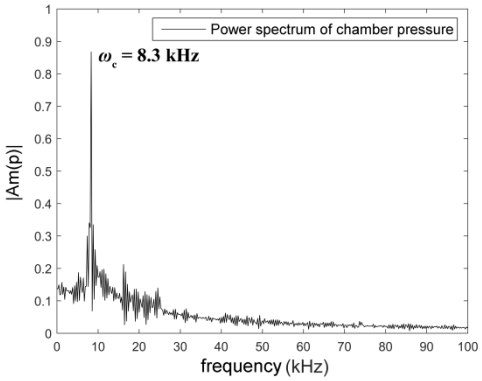

Figure 3. Power spectral densities of CBT data

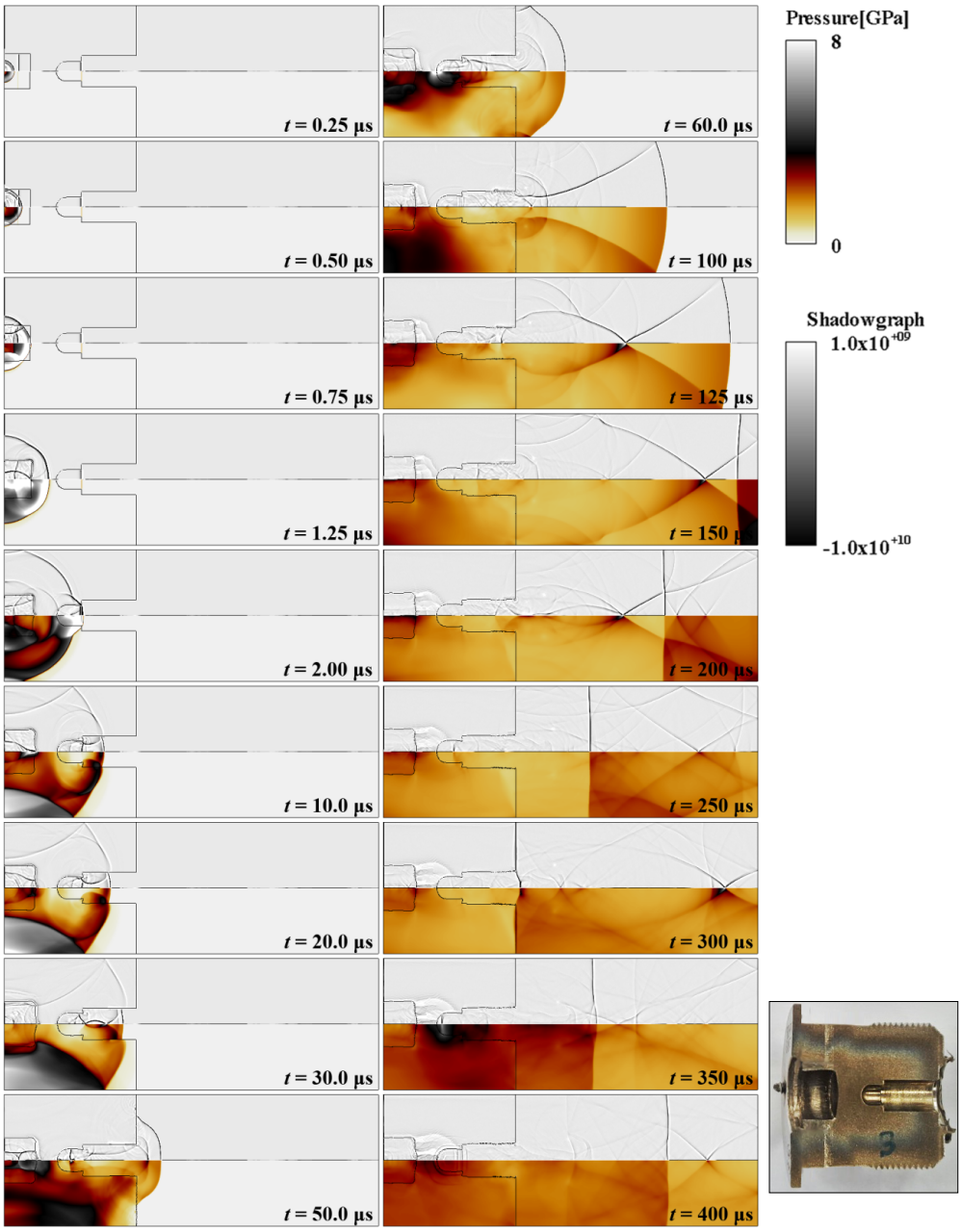

Figure 4. Shown schlieren (top) and pressure (bottom) fields for entire PMD-chamber assembly that shows the detonator (HNS+HMX), bulkhead (STS), acceptor (RDX), and propellant ($BKNO_3$). Right lower corner is a cross cut of the actual device after single use for comparison with numerical prediction of deformed boundaries.

Figure 4 shows that reactive flow motion generated by the pyrotechnic initiator composed of detonator (HNS+HMX) / bulkhead (STS) / acceptor (RDX) / pyrotechnic propellant ($BKNO_3$) flowed into a 10 cc enclosed chamber. The initiation of energetic materials was derived considering the bulkhead thickness of

3.8 mm. The explosive train consisting of detonator, bulkhead and acceptor completes its reaction in about 2.0 μs.

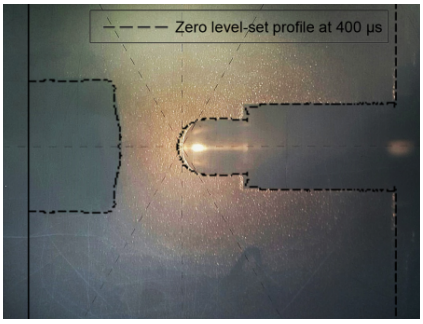

Figure 5. Shape comparison of deformed boundaries of STS with zero level-set lines

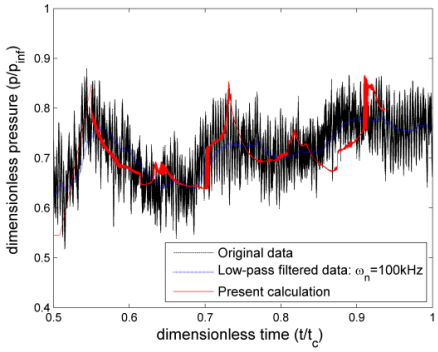

Figure 6. Comparison of pressure fluctuation in CBT

Then, another 40 μs is consumed to fully deflagrate $BKNO_3$. The hot product gas fills the CBT chamber from about 50 μs and on. In the figure, a shadowgraph shown in the upper and pressure is shown in the lower half of each timed image. The release pressure wave into the chamber starts to bounce off of the right-end wall, which is repeating at every 130 μs. This time characteristic is in striking agreement with the dominant frequency measurement from Fig. 3 (ω_c = 8.3 KHz). The dynamic shape change of the stainless casing for donor, acceptor, and propellant is also compared between actual photographic image and numerical result from the level-sets. The donor and acceptor cavities are expanded in all directions due to detonation pressure buildup. The resulting curvature of STS cavities is in good agreement with the simulation result as depicted in Fig. 5. Figure 6 shows the comparison of the pressure fluctuation measured from experiment and calculation in the chamber. One can confirm that the periods of the longitudinal wave motion and maximum peaks in the chamber match quite well.

4 Conclusions

Since the present methodology for analyzing the energetic component system involving detonation of high explosives, deflagration of propellant, and deformation of confinement system is quite straight forward, one needs to properly implement the outlined formulation into a shock physics code for a state-of-the art full scale hydrodynamic simulation involving such energetic components.

Acknowledgment

Authors would like to thank the financial supports from Agency for Defense Development (SW) and Hanwha Corp. (PMD) contracted through the Institute of Advanced Aerospace Technology at Seoul National University.

References

[1] Kim B, Park J, Lee K, Yoh JJ. (2014). A reactive flow model for heavily aluminized cyclotrimethylene-trinitramine. J. App. Phys. 116: 1.

[2] Kim K, Yoh JJ. (2008). Shock compression of condensed matter using multimaterial reactive ghost fluid method. J. Math. Phys. 49: 1.

[3] Kim B, Park J, Yoh JJ. (2016). Analysis on shock attenuation in gap test configuration for characterizing energetic materials. J. App. Phys. 119: 1.

[4] Fried LE, Howard WM, Souers PC. Cheetah 2.0 User's Manual. UCRL-MA-117541, LLNL, 1998.

[5] Lee HS. (2009). Ignition delay investigation in a Pyrotechnic Cartridge. AIAA 2009-5191: 1.